中国激光

基于表面曲线光栅的高功率窄线宽半导体激光器

唐慧，李瑞冬，邹永刚*，田锟，郭誉钧，范杰

长春理工大学高功率半导体激光国家重点实验室，吉林 长春 130022

摘要 随着智能感知技术的快速发展，高功率、窄线宽的半导体激光光源成为研究热点。通过在边发射半导体激光器件表面引入高阶曲线光栅，设计了一种独特的非稳谐振腔结构，可实现高功率和窄线宽。采用紫外光刻和电感耦合等离子体（ICP）刻蚀技术，制备了周期为 6.09 μm、占空比为 0.66、刻蚀深度为 500 nm 的曲线光栅。在室温条件下，测得腔长为 2 mm 的器件的阈值电流为 220 mA，连续输出功率为 1.48 W，斜率效率为 0.63 W/A。比较了法布里-珀罗激光器、直线光栅分布式反馈（DFB）激光器和曲线光栅 DFB 激光器的光谱，结果表明，曲线光栅对半导体激光器的模式选择起到了关键作用，有利于实现高功率 DFB 激光器的窄线宽单模输出。该器件具有制作工艺相对简单、性能优异、可靠性高等特点，具有广阔的应用前景。

关键词 激光器；半导体激光器；曲线光栅；高阶光栅；高功率；窄线宽

中图分类号 TN365 **文献标志码** A **DOI**：10.3788/CJL221148

1 引 言

结构紧凑、寿命长、电光转换效率高、可直接调制的半导体激光器被广泛应用于固体和光纤激光器、激光通信、激光雷达及医疗诊断等领域[1-2]。智能感知技术的快速发展和核心器件的更新换代对激光光源提出了更窄的光谱线宽和更高的输出功率[3]要求。

典型的窄线宽半导体激光器采用集成光栅结构[4]，如分布布拉格反射（DBR）或分布式反馈（DFB）半导体激光器，与外腔激光器相比，其具有高集成度和低成本等明显优势[5]。制备时通常采用掩埋式光栅，制备过程中的二次外延生长工艺难度高，耗时长，增加了器件的制作周期和成本[6]。为了解决这一问题，研究者提出了在器件中采用表面光栅的方案。据文献[7-9]报道，表面光栅 DFB 激光器具有优异的工作特性[高功率、窄线宽、大的边模抑制比（SMSR）、小温漂等]。一般来说，增加脊宽度是增加器件输出功率的相对直接的方法。然而，对于宽脊 DFB 激光器，需要引入额外的高阶横模抑制机制，以确保器件的单模高功率运行。非稳腔激光器是将非稳定谐振腔与宽条形半导体激光器结合起来[10]，使器件具有高度的侧向模式选择性，从而获得良好的线宽。经过多年的探索和实验，非稳腔激光器的诸多卓越性能得到了体现和证实[11]。目前，非稳腔激光器可实现 0.18 nm 的光谱线宽及 1 W 的功率输出[12]。然而，这一概念主要被用于气体和固体激光器的设计与研究，而传统非稳腔半导体激光器的制作过程涉及复杂的曲线腔面工艺，如侧面抛光、深刻蚀、离子束铣削、离子束研磨等[13-15]，导致制备成本高、难度大，难以实现实用化和工程化。因此，开展非稳腔半导体激光器研究，设计易于制备的新型非稳腔激光器，提升器件输出性能仍是非常有挑战的课题。

本文研究了一种含有高阶曲线光栅的非稳腔半导体激光器。具有宽电流注入区的曲线光栅结构不仅增加了不同振荡模式间的损耗差异，提高了模式分辨能力，还可以获得比传统窄脊基横模激光器更大的增益和功率。该器件实现了稳定的单纵模激光发射，输出功率较大，线宽较窄，且制备过程仅需要标准紫外光刻和常规电感耦合等离子体（ICP）刻蚀技术，不需要二次外延或纳米级光栅的复杂技术，低成本和简单的制备工艺增强了其商业化的潜力[16]。

2 结构设计及制备

针对 980 nm 波段的半导体激光器，依据 III-V 族三元化合物材料体系的发光波长范围，选取 InGaAs/GaAs 为有源区量子阱材料。设计了非对称厚度的 AlGaAs 波导结构。对于限制层结构，通过增大铝组分减小该层折射率，当光发生全反射时，光场集中在波导层内。利用金属有机化合物化学气相沉积（MOCVD）法在 GaAs 衬底上生长器件外延层结构，制得表面均匀的外延片[图 1(a)]，并采用光致发光（PL）光谱仪测

收稿日期：2022-08-15；**修回日期**：2022-09-17；**录用日期**：2022-10-17；**网络首发日期**：2022-11-04

基金项目：吉林省科技发展计划项目（20190302052GX，20210201030GX）

通信作者：*zouyg@cust.edu.com

试分析外延材料的发光特性。选取中心点进行单点测试，外延片光致发光光谱波长(λ)为966.7 nm，半峰全宽为25.8 nm，如图1(b)所示。由于光致发光测试是在常温下进行，但半导体激光器在注入电流温度升高时，波长会发生红移，因此制得的外延片满足980 nm曲线光栅DFB半导体激光器的波段要求。

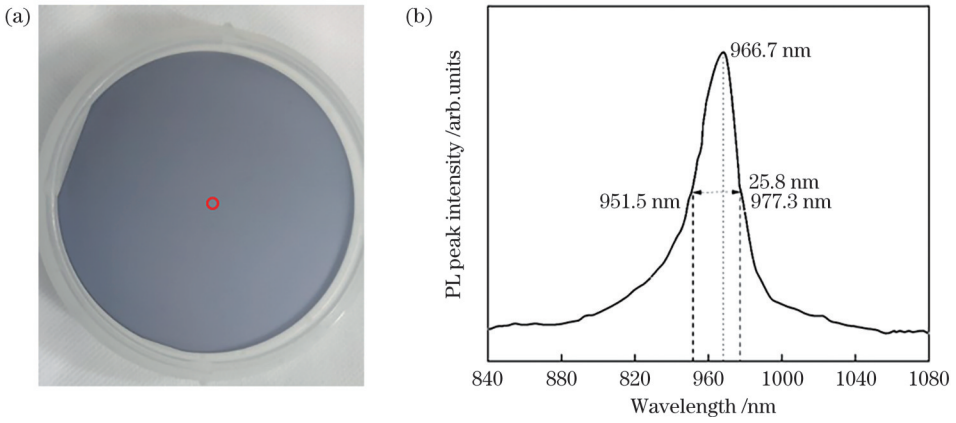

图1　MOCVD法生长的外延片及PL测试结果。(a)外延片；(b)PL测试结果

Fig. 1　Epitaxial wafer grown by MOCVD and PL test result. (a) Epitaxial wafer; (b) PL test result

图2所示为脊波导中基模、一阶模和二阶模下的光场强度分布，其中脊宽(W_r)为400 μm。在侧向上，相比于高阶模，基模的光场更多分布在靠近波导中间的位置；一阶侧模为双瓣，主要分布在宽脊波导两侧；二阶侧模为三瓣，能量分布更加分散[17]。宽脊波导激光器在高功率输出状态下模式竞争激烈，输出模式数目多，造成其近场光斑呈现出“多瓣”现象，影响其应用范围。基于光场强度分布，我们设置电流注入区和非注入区，即图2中的白色和灰色区域，这两个区域分别为增益区和损耗区。通过计算宽脊波导中常见的几种横模，设置不同横模(侧模)间的有源区光限制因子差，实现对模式的选择。高阶侧模比基模具有更小的增益和更大的损耗而被抑制。侧向基模具有比高阶侧模更低的损耗，这也是模式的场分布决定的，从而增强了非

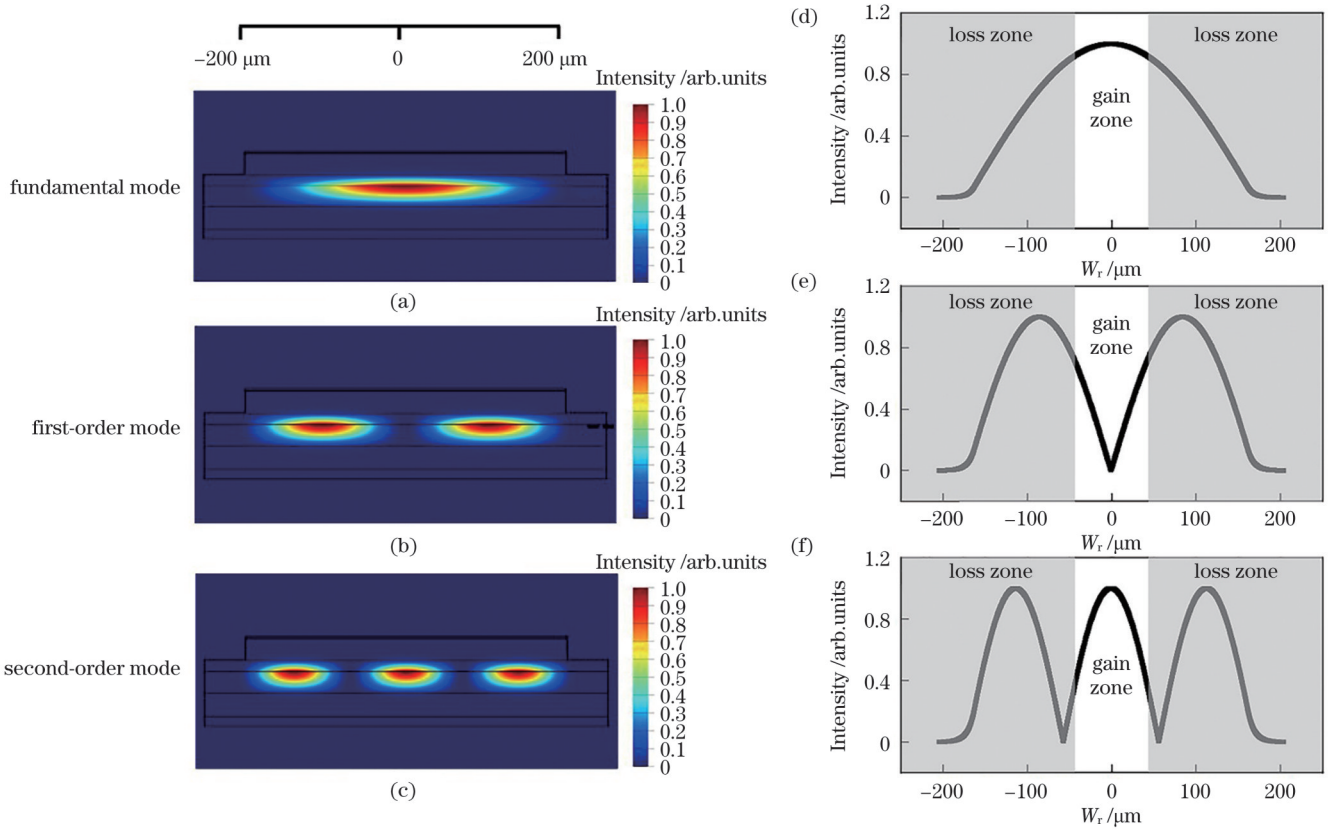

图2　不同模式下的光场分布及归一化光场强度分布。(a)～(c)光场分布；(d)～(f)归一化光场强度分布

Fig. 2　Light field distributions and normalized intensity distributions of light field under different modes. (a)–(c) Light field distribution; (d)–(f) normalized intensity distributions of light field

稳定谐振腔调控侧模的作用，提高了器件的模式识别能力，可实现器件高功率基模的稳定输出。

曲线光栅的曲率半径$R(x)$满足

$$\frac{4}{R(x)}=\frac{1}{L+x}-\frac{1}{L-x},\tag{1}$$

式中：L为腔长；x为与后腔面的距离。

如图3所示，非稳腔激光器为半对称结构[18]，由一个平坦的高反射镜和一个弯曲的输出镜组成，输出光束在非稳腔内不断来回振荡反射，波面横向尺寸逐渐增大。器件的腔长为2 mm，脊宽W_r和脊高分别为400 μm和1.2 μm。光栅的半径与其位置（即x）相关，从后腔面往前腔面方向逐渐减小。从y方向看，光栅周期从中间到边缘逐渐增大，其中灰色区域为需要刻蚀的光栅槽，中间深色区域为P电极电流注入区。可以看到，在电流注入区的位置，光栅几乎是直线型光栅，周期变化非常小，因此，这种激光器的结构设计可参考熟知的直线型光栅激光器的仿真结果。

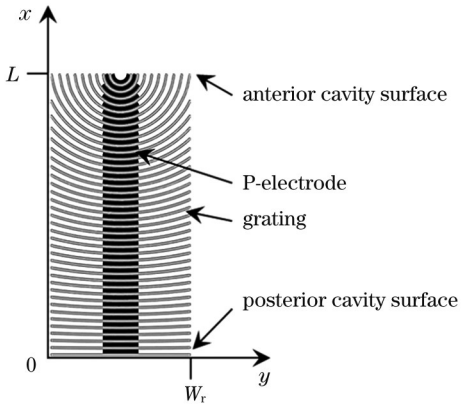

图3　高阶曲线光栅非稳腔示意图

Fig. 3　Schematic of unstable cavity with high-order curved grating

利用高阶曲线光栅结构形成的非稳腔，其独特之处在于光栅是弯曲的，使光束具有发散性，几何偏折损耗大，从而增加了不同振荡模式间的损耗差异，提高了模式分辨能力，因此容易抑制高阶模，输出最低阶的基模，并在一定范围内较好地限制和控制光谱线宽[19]。其次，较大的脊宽使得器件获得了较大面积的均匀增益。此外，光线在每次反射时都会产生一条新的路径，从而避免了自聚焦效应引起的光丝[20]。

曝光光栅图形是制备高阶曲线光栅的关键工艺之一，光栅和P电极被依次图案化处理。由于结构的微米尺度，采用标准紫外光刻和普通电感耦合等离子体刻蚀技术制备该器件。与电子束光刻相比，紫外光刻成本低，制造工艺简单，在实际生产中更实用。图4为显影后通过金相显微镜观察到的曲线光栅，其形貌清晰、对比明显。

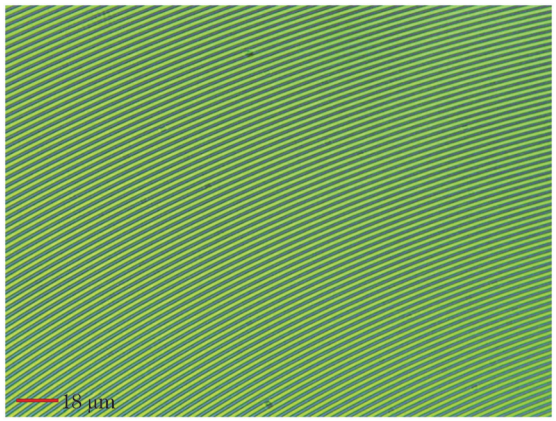

图4　曲线光栅掩模图

Fig. 4　Curved grating mask pattern

采用ICP刻蚀技术对带有光刻胶掩模的外延片进行干法刻蚀，刻蚀参数如下：刻蚀气体Cl_2的流量为10 mL/min，BCl_3的流量为20 mL/min，Ar的流量为30 mL/min。为了摸索出稳定的刻蚀速率并优化光栅形貌，我们对光栅进行了过度刻蚀，刻蚀时间为120 s，光栅深度为2.08 μm，所得刻蚀速率为17.3 nm/s。在正式流片时，光栅的刻蚀深度为500 nm，刻蚀时间设置为29 s。如图5所示，在扫描电子显微镜（SEM）下观察到周期为6.09 μm、占空比为0.66、刻蚀深度为2.08 μm的高阶曲线光栅，光栅条纹清晰、完整，具有陡直的侧壁形貌及良好的周期性和均匀性。

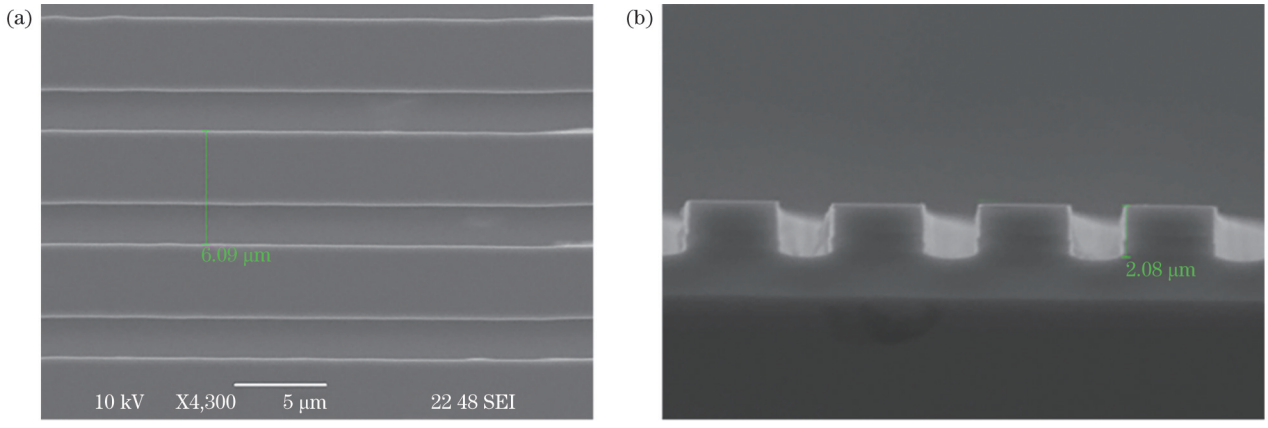

图5　曲线光栅的SEM图。(a)表面图；(b)侧壁图

Fig. 5　SEM images of curved grating. (a) Surface view; (b) side wall view

使用等离子体增强化学气相沉积(PECVD)设备在外延片上沉积厚度约为500 nm的SiO_2介质膜作为电绝缘隔离层,阻止电极窗口以外区域的电流注入。再在二氧化硅隔离层上进行紫外光刻,曝光出P电极窗口图形后,选用缓冲氧化物刻蚀液湿法腐蚀电极窗口下的SiO_2。用台阶仪测量其腐蚀深度,观察电极窗口区域的SiO_2是否被完全腐蚀干净且未发生侧向腐蚀,避免电极窗口处注入电流向脊外扩散。利用磁控溅射技术在外延片P电极上溅射30 nm厚的Ti膜层、30 nm厚的Pt膜层和300 nm厚的Au膜层。最底层为金属Ti,与外延片表面接触,主要起到黏附作用;中间层为金属Pt,阻挡Au层向外延片内部扩散,降低激光器的光电转换效率;最上层为Au层,其具有良好的导电作用。在P电极剥离后,开始进行减薄、抛光处理,利用自动研磨机"少时多磨",将外延片减薄至厚度为140 μm左右,用抛光机抛光外延片3 min左右后,清洗干净,利用磁控溅射技术溅射N电极,依次溅射5 nm厚的Ni膜层、100 nm厚的AuGe膜层、45 nm厚的Ni膜层和300 nm厚的Au膜层。

为了降低半导体激光器的电阻,将外延片放入快速退火炉中进行合金退火处理,设置温度为420 ℃,时间为60 s。退火时将水冷温度控制在15.5 ℃,循环水温度控制在19.9 ℃,并在合金退火过程中通入流速稳定的N_2。再利用解理机解理出高阶曲线光栅DFB半导体激光器巴条,用电子束镀膜机镀制增透膜(反射率约为5%)和高反膜(反射率约为99.5%)。最后,解理出高阶曲线光栅DFB半导体激光器单管,其腔长为2 mm、脊宽为400 μm,并采用COS(chip on submount)封装方式将其封装在热沉上,用金丝球焊机进行引线,完成贴片的器件如图6所示。

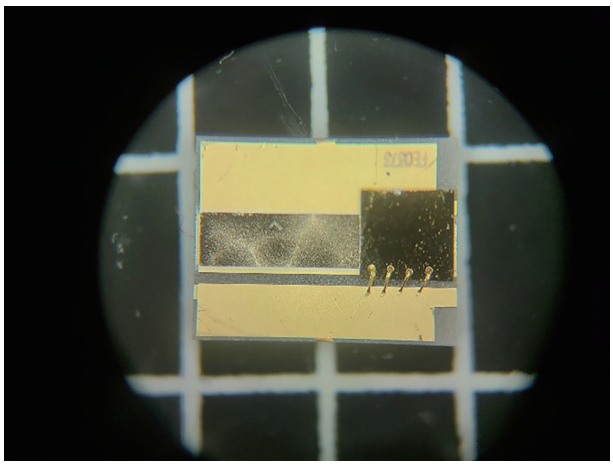

图6　COS封装曲线光栅半导体激光器

Fig. 6　COS packaged curved grating semiconductor laser

3　测试分析

为了对比分析,在曲线光栅半导体激光器的制备过程中,采用同一外延片同时制备了F-P激光器和宽脊直线型光栅DFB激光器。图7所示为室温条件下连续工作模式的法布里-珀罗(F-P)激光器、直线光栅DFB激光器和曲线光栅DFB半导体激光器的功率-电流-电压(*P-I-V*)测试结果。对于曲线光栅DFB半导体激光器,其阈值电流为220 mA。在电流从0增加到2.5 A的过程中,阈值电流以下时激光器的输出功率低至可忽略不计,阈值电流以上时输出功率接近线性增加。当注入电流为2.5 A时,电压为2.11 V,器件连续输出激光功率为1.48 W,经计算斜率效率为0.63 W/A。较低的斜率效率是非稳腔激光器的损耗机制引起的,光在腔内有限次往返后,会有部分光逸出腔外,造成较大的损耗,因此这种腔也被称为高损耗腔。随着注入电流逐渐增加,器件的斜率效率略微降低,这是大电流注入情况下激光器腔内温度升高造成的。与曲线光栅DFB激光器相比,F-P激光器的阈值电流较小,约为120 mA,直线光栅DFB激光器的阈值电流为230 mA,这是因为DFB器件中的高阶表面光栅引入了辐射损耗,增加了激光器的阈值增益。当注入电流为2.5 A时,F-P激光器和直线光栅DFB激光器的输出功率分别为2.5 W和1.1 W。DFB激光器的斜率效率和输出功率都不如F-P激光器,这是因为表面光栅的辐射损耗导致了功率损失。在同一注入电流条件下,直线光栅DFB激光器的输出功率略小于曲线光栅DFB激光器。

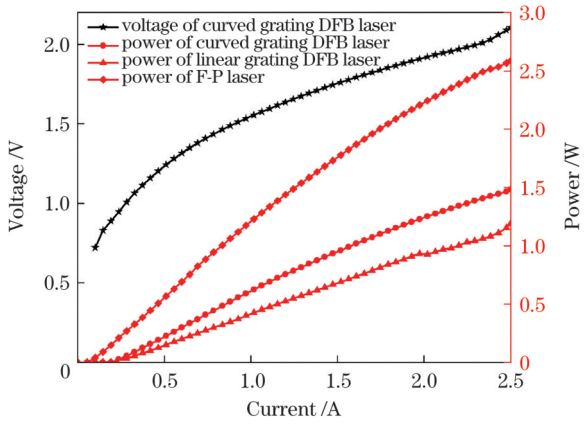

图7　不同激光器的*P-I-V*特性

Fig. 7　*P-I-V* characteristics of different lasers

利用光谱仪测试获得的器件光谱图如图8所示。可以看出,单纵模激射光谱均表现良好,光谱线宽分别为0.117、0.145、0.132 nm,边模抑制比分别为23.5 dB、28 dB、28.4 dB,器件激射波长(λ)分别为979.76、980.07、980.4 nm。随着注入电流的增大,器件的输出波长向长波长方向漂移,漂移速率为6.4 nm/A。这是器件内部的温度升高,尤其是有源区温度的升高引起禁带宽度变窄及折射率增加造成的。

在1 A的工作电流下,腔长为2 mm的F-P激光器、直线光栅DFB激光器和曲线光栅DFB激光器的光谱图如图9所示。

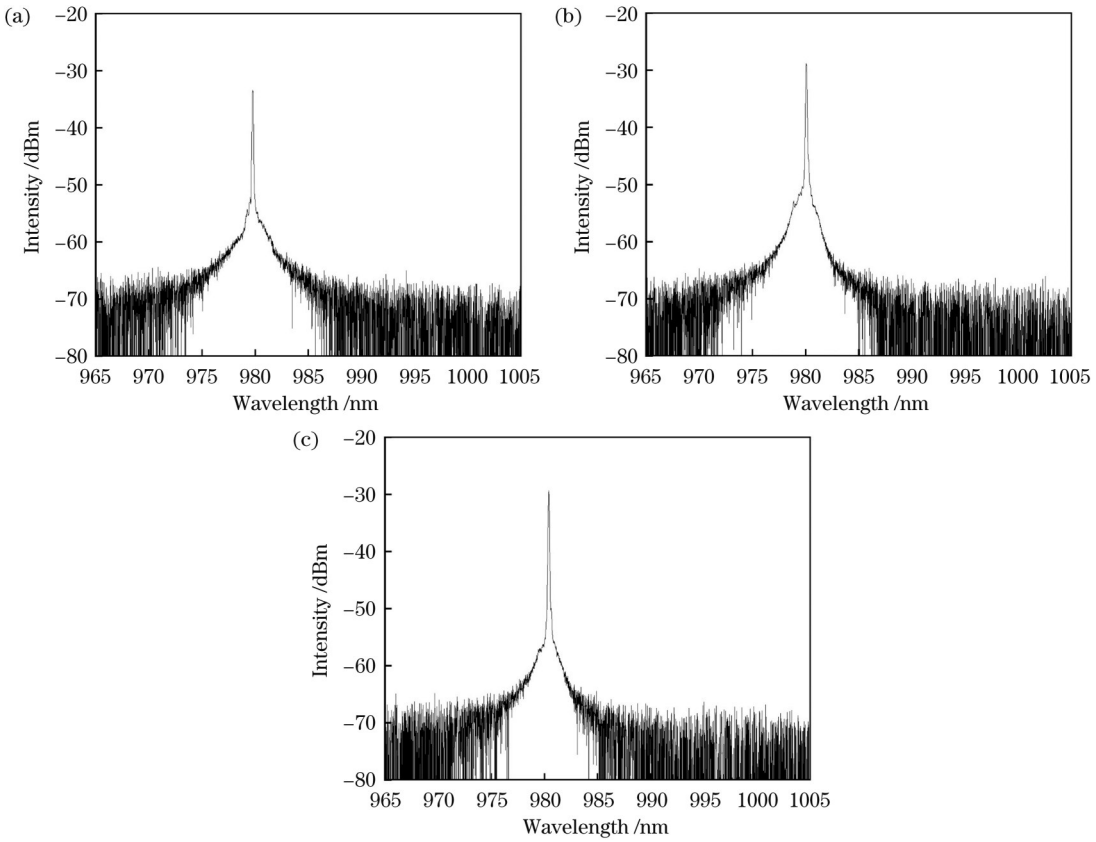

图 8　不同注入电流下曲线光栅边发射 DFB 半导体激光器的光谱图。(a) 450 mA；(b) 500 mA；(c) 550 mA

Fig.8　Spectra of curved grating edge-emitting DFB semiconductor lasers under different injection currents. (a) 450 mA; (b) 500 mA; (c) 550 mA

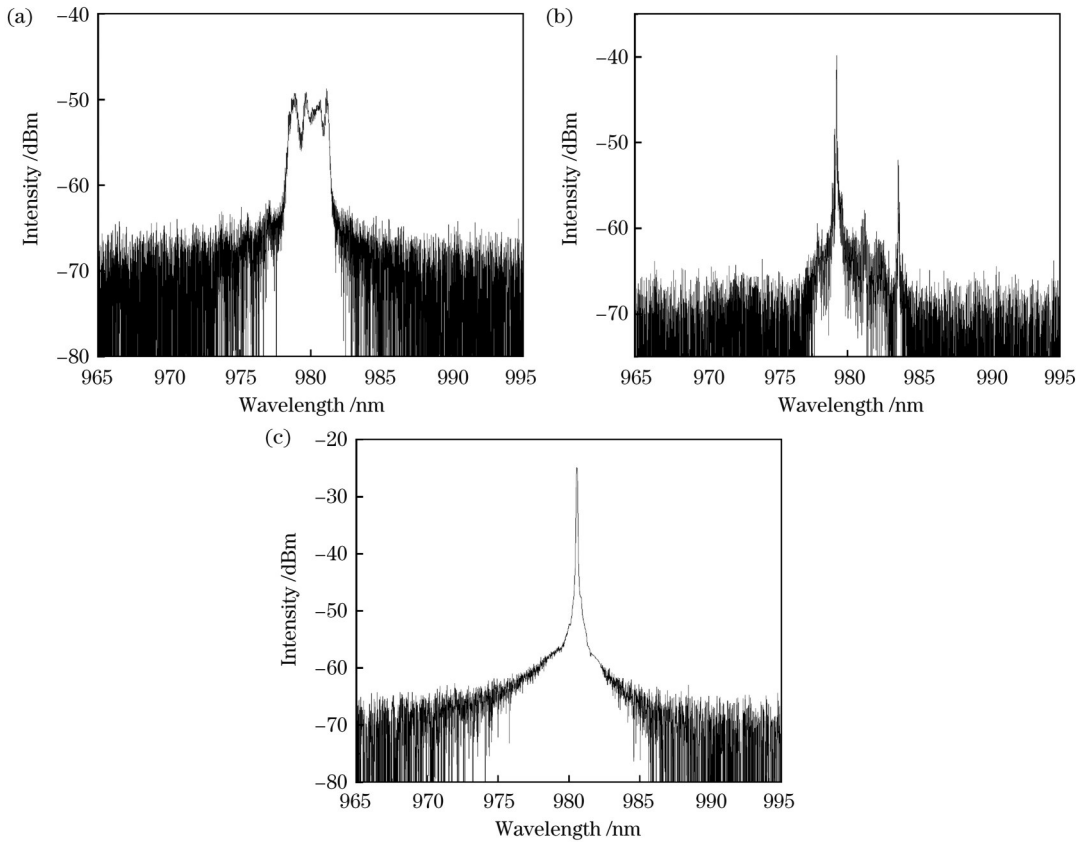

图 9　不同激光器的光谱图。(a)F-P 激光器；(b)直线光栅 DFB 激光器；(c)曲线光栅 DFB 激光器

Fig.9　Spectra of different lasers. (a) FP laser; (b) linear grating DFB laser; (c) curved grating DFB laser

F-P激光器光谱宽度大约为1.7 nm，约为曲线光栅器件的14倍，这是因为腔内有效折射率会受到器件自热效应和等离子体效应的影响，激射波长出现跳变现象，所以多纵模同时激射，光谱线宽较宽。直线光栅DFB激光器依靠光栅对光进行选频，使其产生振荡，只有满足Bragg条件的波长在激光器中才能引起稳定振荡，起到选纵模、压缩线宽的作用。因此相较于F-P激光器，直线光栅DFB激光器能实现稳定的单纵模输出，但光谱仍存在次峰，其原因是在大电流注入条件下，增益空间烧孔和光成丝导致了腔内多模激射。而曲线光栅激光器波长为980.55 nm，光谱线宽为0.121 nm，边模抑制比为32 dB，由此可见，曲线光栅实现了对半导体激光器的模式选择，有利于实现高功率DFB激光器的窄线宽单模运转。这种高阶曲线光栅DFB激光器的制备只需标准紫外光刻技术即可实现，不需要复杂且昂贵的电子束光刻技术及二次外延技术，将在高功率半导体激光器领域中具有良好的应用价值。

4 结　论

设计并制备了一种基于高阶表面曲线光栅的非稳腔半导体激光器，其具有线宽窄、功率高、单模出光的优良性能。在室温条件下，腔长为2 mm的器件的阈值电流为220 mA，连续输出功率为1.48 W，斜率效率为0.63 W/A。通过比较法布里-珀罗激光器、直线光栅DFB激光器和曲线光栅DFB激光器的光谱，证实了曲线光栅对半导体激光器的模式选择的关键作用，该作用有利于高功率DFB激光器的窄线宽单模工作，其在注入电流为1 A时的激射波长为980.55 nm，光谱线宽为0.121 nm，边模抑制比为32 dB。这种激光器为大规模生产高功率、窄线宽、波长稳定的DFB半导体激光器提供了一种解决方案。相比于传统的DFB激光器，其具有制作工艺简单的优点，在激光切割、焊接、熔覆，激光医疗，激光雷达，光通信等领域中具有非常广阔的应用前景。

参 考 文 献

[1] 柯旭，邓乐武. 弱耦合互注入锁定半导体激光器的线宽研究[J]. 中国激光，2022，49(3)：0301001.
Ke X，Deng L W. Linewidth of mutually injection-locked semiconductor lasers in weak coupling regime[J]. Chinese Journal of Lasers，2022，49(3)：0301001.

[2] 袁庆贺，井红旗，刘素平，等. 导波模式对锥形半导体激光器输出特性的影响[J]. 中国激光，2021，48(9)：0901001.
Yuan Q H，Jing H Q，Liu S P，et al. Influence of guided wave mode on output characteristics of tapered diode laser[J]. Chinese Journal of Lasers，2021，48(9)：0901001.

[3] 程乃俊，李惟帆，祁峰. 中红外激光器研究进展[J]. 激光与光电子学进展，2023，60(17)：1700006.
Cheng N J，Li W F，Qi F. Progress of mid-infrared laser[J]. Laser & Optoelectronics Progress，2023，60(17)：1700006.

[4] 张蕾. 微集成窄线宽半导体激光器仿真设计与线宽测试[J]. 光学与光电技术，2021，19(1)：42-47，60.
Zhang L. Simulation design and linewidth test on narrow linewidth semiconductor laser device[J]. Optics & Optoelectronic Technology，2021，19(1)：42-47，60.

[5] 齐军，邹永刚，范杰，等. 1064 nm侧向微结构宽脊波导半导体激光器[J]. 中国激光，2021，48(13)：1301003.
Qi J，Zou Y G，Fan J，et al. 1064 nm wide-ridge waveguide semiconductor laser with lateral microstructure[J]. Chinese Journal of Lasers，2021，48(13)：1301003.

[6] Uusitalo T，Virtanen H，Dumitrescu M. Transverse structure optimization of distributed feedback and distributed Bragg reflector lasers with surface gratings[J]. Optical and Quantum Electronics，2017，49(6)：206.

[7] Gao F，Qin L，Chen Y Y，et al. Study of gain-coupled distributed feedback laser based on high order surface gain-coupled gratings[J]. Optics Communications，2018，410：936-940.

[8] Hou C C，Chen H M，Zhang J C，et al. Near-infrared and mid-infrared semiconductor broadband light emitters[J]. Light：Science & Applications，2018，7(3)：17170.

[9] Wei S Z，Sun W，Lu Q Y，et al. Design of 2.3 μm low threshold single mode GaSb DBR lasers based on high order slotted surface grating[J]. Proceedings of SPIE，2021，11763：117638I.

[10] 刘莹，范杰，齐军，等. 侧向非对称光栅光场耦合特性的理论研究[J]. 光学学报，2021，41(8)：0823020.
Liu Y，Fan J，Qi J，et al. Theoretical study on light field coupling of lateral asymmetric gratings[J]. Acta Optica Sinica，2021，41(8)：0823020.

[11] Ongstad A P，Dente G C，Tilton M L，et al. High brightness from unstable resonator mid-IR semiconductor lasers[J]. Journal of Applied Physics，2010，107(12)：123113.

[12] Garrod T J，Olson D，Xiao Y，et al. Long wavelength surface-emitting distributed feedback (SE-DFB) laser for range finding applications[J]. Proceedings of SPIE，2012，8241：824113.

[13] Srinivasan S T，Schaus C F，Sun S Z，et al. High-power spatially coherent operation of unstable resonator semiconductor lasers with regrown lens trains[J]. Applied Physics Letters，1992，61(11)：1272-1274.

[14] Bao Z，Defreez R K，Carleson P D，et al. Design considerations for high-power GaInP/AlGaInP unstable-resonator semiconductor lasers[J]. Applied Optics，1993，32(36)：7402-7407.

[15] O'Brien P，Moorhouse C，Braddell J，et al. Imaging of curved facet unstable resonator semiconductor lasers operating at 980 nm [J]. Electronics Letters，1998，34(6)：561-562.

[16] Liu Y X，Yang G W，Wang Z F，et al. High-power operation and lateral divergence angle reduction of broad-area laser diodes at 976 nm[J]. Optics & Laser Technology，2021，141：107145.

[17] Lei Y X，Chen Y Y，Gao F，et al. 990 nm high-power high-beam-quality DFB laser with narrow linewidth controlled by gain-coupled effect[J]. IEEE Photonics Journal，2019，11(1)：1500609.

[18] Tilton M L，Dente G C，Paxton A H，et al. High power，nearly diffraction-limited output from a semiconductor laser with an unstable resonator[J]. IEEE Journal of Quantum Electronics，1991，27(9)：2098-2108.

[19] Hamana K，Das P K，Omachi O，et al. GaInP/AlGaInP quantum well distributed Bragg reflector laser using surface curved grating [J]. Japanese Journal of Applied Physics，2004，43(2)：642-643.

[20] Kanskar M，Cai J，Kedlaya D，et al. High-brightness 975-nm surface-emitting distributed feedback laser and arrays[J]. Proceedings of SPIE，2010，7686：76860J.

High-Power Narrow-Linewidth Semiconductor Laser Based on Surface Curved Gratings

Tang Hui, Li Ruidong, Zou Yonggang*, Tian Kun, Guo Yujun, Fan Jie

State Key Laboratory of High Power Semiconductor Laser, Changchun University of Science and Technology, Changchun 130022, *Jinlin, China*

Abstract

Objective Semiconductor lasers with compact structure, long life, high electro-optical conversion efficiency, and direct modulation are ideal for many traditional applications. The rapid development of intelligent sensing technology and the replacement of core devices have resulted in higher performance requirements of narrower spectral linewidth and higher output power for such lasers. The typical solution for realizing narrow-linewidth semiconductor lasers is the implementation of buried gratings. However, the necessary secondary epitaxial growth in the fabrication is difficult and time-consuming; it also leads to increased fabrication cycle time and cost of the device. The use of surface gratings in the devices has been proposed to address this issue. Prior studies indicate that distributed feedback (DFB) lasers based on surface gratings exhibit excellent operating characteristics [e. g. , high power, narrow linewidth, large side-mode suppression ratio (SMSR), and small temperature drift]. In general, increasing the ridge width is a relatively straightforward method of increasing the output power of the device. However, for wide-ridge DFB lasers, additional high-order transverse mode suppression mechanisms must be introduced to ensure single-mode high-power operation of the device. An unstable cavity laser is the combination of unstable resonator and wide stripe semiconductor laser, which renders the device as exhibiting high lateral mode selectivity. Consequently, it can provide good linewidth in broad area lasers. However, the structures of unstable cavity semiconductor lasers are diverse and complex, with most using electron beam lithography, holographic lithography, multi-step etching, secondary epitaxy, and other processes. This results in high manufacturing costs and difficulties; thus, its practical implementation and engineering are challenging. The structural design and characteristic optimization of novel unstable cavity laser are vital and of practical significance for the performance improvement and application expansion of semiconductor lasers. This study examined an unstable cavity semiconductor laser with high-order curved gratings. The use of curved grating with a wide current injection region increases the loss difference between different oscillation modes and improves the mode discrimination such that it can obtain greater gain and power than the conventional narrow-ridge fundamental transverse mode lasers.

Methods There are four main aspects to the methodology employed. 1) The device adopts a wide ridge structure for high power output of the device. The broad-area ridge structure enables the fundamental mode in the cavity to exhibit a larger mode volume, which facilitates the extraction of increased gain and power than conventional narrow-ridge fundamental transverse mode lasers. Moreover, the broad-area ridge reduces the power density and thermal load of the device and improves the stability of the laser. 2) Through the setting of the gain and non-gain regions on the ridge, the high-order side mode is suppressed. The parameters of current injection/non-injection regions in the ridge are set to suppress high order lateral modes. Further, the energy of the fundamental mode distributed in the gain region is greater than those of the first- and second-order modes distributed in the gain region. Consequently, the fundamental mode obtains a larger gain than the high-order mode, which is beneficial to the stable operation of the device under the fundamental mode. 3) The curved grating and the high reflective rear facet form an unstable cavity, which enhances the mode discrimination of the resonator and realizes the single-mode stable output of the device. The unstable cavity for mode selection is formed owing to the highly reflective rear facet and curved gratings that are defined by standard ultraviolet lithography. The structural design of the curved grating exhibits remarkable flexibility, which considerably reduces the difficulty and complexity of device design and fabrication. In addition, lateral modes regulated by curved gratings in the broad area device strengthen the mode discrimination and enhance the device's ability to suppress spatial gain hole burning and filamentation. 4) High-order curved gratings are used to achieve selection of wavelengths in the cavity. A high-order grating is used to realize the distributed feedback of light in the cavity. Compared with the low-order grating, the designing and manufacturing are less challenging, and the cost is lower.

Results and Discussions The experimental results show that the threshold current, continuous output power, and slope efficiency of the curved grating semiconductor laser device are 220 mA, 1.48 W, and 0.63 W/A, respectively (Fig. 7). The single longitudinal mode lasing spectra of the devices under the injection current of 450, 500, and 550 mA all exhibit good performance. With the increase of the current, the spectral linewidths are obtained as 0.117, 0.145, and 0.132 nm, respectively, and the side mode suppression ratio are 23.5 dB, 28.0 dB, and 28.4 dB, respectively. Further, the laser wavelengths of the device are 979.76, 980.07, and 980.4 nm, respectively. With increase in the injection current, the output wavelength of the device drifts to the long wavelength direction at a drift rate of 6.4 nm/A (Fig. 8). Through comparisons of the spectra of Fabry-Perot, linear grating DFB, and curved grating DFB lasers, the critical role of curved gratings in mode selection of semiconductor lasers is demonstrated. It is therefore beneficial to realize the narrow-linewidth single-mode operation of high-power DFB lasers with a lasing wavelength of 980.55 nm, a

spectral linewidth of 0.121 nm, and a side-mode suppression ratio of 32 dB at an injection current of 1 A (Fig. 9).

Conclusions This study proposes the fabrication of a novel broad-area distributed feedback laser with high order surface curved gratings based on standard ultraviolet lithography. The high-order curved grating is used to form an unstable cavity structure, which increases the loss difference between different oscillation modes, improves the mode discrimination, and obtains uniform gain over a broad area. The DFB laser emitting at wavelength of approximately 980.55 nm achieves a spectral width of 0.121 nm and maximum output power of 1.48 W. The threshold current and sidemode suppression ratio of the device are 220 mA and 32 dB, respectively. Further, through comparisons of the power-current-voltage curves and spectra of Fabry-Perot, linear grating DFB, and curved grating DFB lasers, it is demonstrated that curved gratings play a key role in power output and mode selection in semiconductors lasers; this finding is beneficial for the realization of narrow-linewidth single-mode operation of high-power DFB lasers.

Key words lasers; semiconductor laser; curved gratings; high-order gratings; high power; narrow linewidth